ISSN 0018-151X, High Temperature, 2016, Vol. 54, No. 5, pp. 627–631. © Pleiades Publishing, Ltd., 2016.
Original Russian Text © A.E. Balanovskii, 2016, published in Teplofizika Vysokikh Temperatur, 2016, Vol. 54, No. 5, pp. 663–668.

PLASMA INVESTIGATIONS

Visualization of the Process of Metal Heating and Melting in the Anode Zone in an Arc Discharge with a Tungsten Electrode

A. E. Balanovskii

Irkutsk National Research Technical University, Irkutsk, 664074 Russia
e-mail: fuco.64@mail.ru

Received July 3, 2015

Abstract—Pictures of an electric arc burning in argon, obtained by means of a digital camera, within the different domains of wavelengths of the visible spectrum are presented. Maps of the thermal fields of the heating spot are plotted, and the plasma temperature in the anode arc zone is calculated. The application potential of the digital image technology in the visible wavelength domain for analysis of the processes directly in the anode arc zone and for estimation of the arc column parameters is shown.

DOI: 10.1134/S0018151X16050060

INTRODUCTION

Arc discharge is an efficient source of metal heating and melting; it has a wide range of scientific and technological applications [1–4]. The technology of the arc discharge applications includes welding, surfacing, cutting, and metal and alloy sputtering. Recently, interesting data have been obtained when studying the anode processes in a vacuum arc [4, 5], in low-temperature plasma generators, and in freely burning arcs [6–9]. To enhance the technique of the electrode material transfer in the welding arc, further investigations of the arc burning stability in all spatial positions are needed; improvement of the welded seam formation by means of objective estimation of the physicochemical state of the metal in the weldpool should be accomplished. Use of digital cameras is a relatively accessible method of online visualization of the processes in the welding arc with obtainment of a rich color palette to adjust and to develop the welding, surfacing, sputtering, and cutting regimes [6–20]. However, the high cost of professional digital cameras limits their application in various technological processes. Recently, enhancement of the digital technology has made it possible to pay attention with the high quality of the images obtained by inexpensive digital cameras that might be accessible to the majority of factories to adjust the welding, surfacing, and sputtering regimes. In this paper, we present the results of visualization of the processes taking place in the welding arc and of the temperature measurements by means of inexpensive digital cameras.

MATERIALS, EQUIPMENT, AND INVESTIGATION TECHNIQUE

In our investigations, the welding arc burned in a protective gas medium, vertically, between a tungsten nonmelting cathode (4 mm in diameter) and a changeable copper or steel anode (Figure 1). The anode surface was plane and polished. The arc was 3 to 15 mm long. The total arc burning duration was equal to 0.1–2 s until formation of the melt metal weldpool. To supply the arc, we engaged the industrial DC welding power supply with an open-circuit voltage of 70 V and a maximal current of 250 A. We varied the current from 5 to 100 A. A high-voltage pulse ignited the discharge in the welding torch. We used high-purity argon as the protective gas. We measured the current and the voltage by means of a Tektronix TDC-1012B digital oscilloscope.

For optical temperature measurement by the brightness pyrometry method, we used inexpensive ά

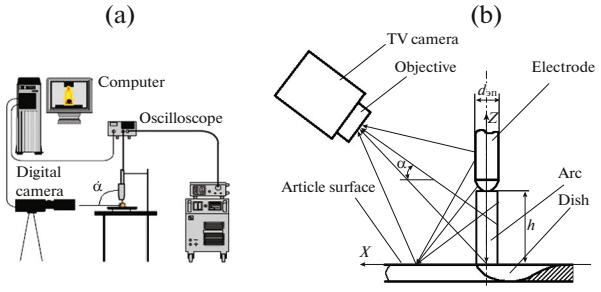

Fig. 1. Experiment layout: (a) general; (b) layout of the ray sources in the welding arc system.

SONY 350 and Canon 550d-18-50 digital mirror cameras. We worked with the cameras as follows. We switched the camera into the manual operating mode and switched off the preliminary processing functions (in particular, noise blanking). Then, we photographed the object, registered the file in the row format, input it into the PC, and transformed it into the TIFF (RGB) format. Next, we wrote each channel of this file as a separate file in the gray (8 bit) TIFF format; the output signal was within 0–255 pixels for each channel. We processed the files using the standard Adobe Photoshop C3 and Lightroom software. We estimated the impartial image quality against the results of the test shooting of the Kodak Q13 test target and of the 65 × 45 cm target (full frame image); here, we also controlled the resolution, the distortion, and the chromatic aberrations. The technique of calibration of the brightness and the color CCD-based pyrometric systems is well developed [10, 11, 14, 15]. We calibrated the digital cameras for the temperature measurements by means of the SI-8 lamp: we varied the filament current of the lamp and registered its temperature. Under such calibration, the resolution in temperature equals 1.2–1.8 K.

In our investigations, we accepted that the measurement errors might be divided into three parts: the systematic errors of the brightness pyrometry method; the errors due to the adjustment; and the direct measurement errors. Thus, we estimated the measurement errors according to the technique of [12, 17, 18]. Our estimate of the error due to establishment of the camera inexactness, the object noise, and the CCD noise equals 4–6 K. The brightness temperature measurement error in our experiments equals 15–30 K. We determined the arc column temperature according to the absolute intensity of the continuum argon spectrum at ArI λ = 480.6 nm. We registered the continuum brightness by means of the PGS-2 spectrograph. We took the carbon arc anode spot, with a known spectral brightness, as the reference. We recalculate the observed arc intensity profiles into the radial densities by solution of the Abel integral equation. To compare the temperature profiles, we used the experimental data [10–12] on the argon emission.

RESULTS

From the standpoint of the experiment methodology, the main problem consisted in the fact that the welding discharge itself, especially at high currents, emits high-power light flux. As a consequence, high-power and essentially irregular, in its volume, emission from the difference gap zones takes place; to registry its pattern, usual means of the light flux limitation should be engaged. These means include work with almost totally closed diaphragms, neutral light filter establishment, and low exposure duration. Nonetheless, a certain compromise is needed because, to obtain the total discharge image, we should examine all zones of the nonstationary emitting interelectrode gap, while the light filters might "cutoff" a sufficient part of the image from the spot located on the melt surface and the fine-scale structures in it.

The arc burning in argon between the tungsten electrode and the mild steel has a transparent column, almost a yellow–white color in the visible emission spectrum. Resulting from the arc action, a melt metal dish with a mirror surface occurs in the main material (Fig. 2). From the moment of arc ignition until the melt metal dish occurrence on the surface, essential differences are observed in the arc behavior. In particular, Fig. 2 shows that at the initial stage of the discharge existence (0.2 s), the arc conjunction is diffusion. Then (0.4 s) the discharge begins to contract to

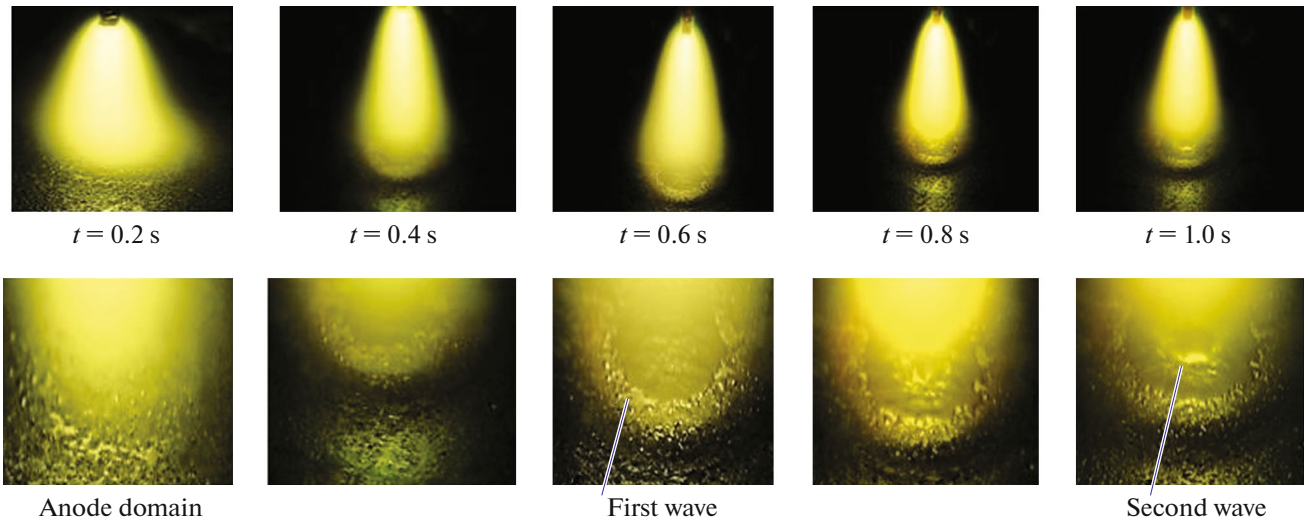

Fig. 2. Visualization of dynamics of the welding arc burning process.

the center, and at 0.6 s, the first portion (the wave) of the molten metal occurs on the anode surface. However, we observe no anode spots in that discharge regime for the given experimental set. Further (Fig. 3), the discharge contracts along the column axis in the anode zone; and the second wave of molten metal occurs. As soon as the second wave of molten metal occurs, the discharge passes into the diffusion regime. At the expense of the hydraulic pressure [6, 7], the second wave shifts the first wave to the heating spot boundary. The second melt wave does not reach the heating spot boundary as the first one does; it stops and produces a clamp; here, the discharge passes to the contracted regime, with occurrence of the well observed anode spots. In the very short arc case, the anode spot moves directly under the electrode, thus giving rise to a voltage drop by about 2–3 V [7, 14, 15]. Such an arc state is unstable [1]. After origin of the second and the third waves of the molten metal, the occurring anode spots begin to move over the melt dish surface extending its volume and involving the deep metal layers into the melting regime. Here, the discharge column itself undergoes a "bottleneck"-like transformation in the anode zone with rejection of the jets from the anode spots (Fig. 3).

For a relatively short arc gap (3 mm), only the arc column is seen in the photographs. For longer arcs (up to 15 mm), two intensive glows occur: the cathode and the anode ones (Fig. 3). With the current increase, the cathode glow intensifies and increases in volume by 5–8%; this fact can be estimated using the criterion of lengthening and widening of the cathode glow domain. Note that with the arc gap increase, at a constant current, the cathode flame remains constant, whereas the anode one elongates. When analyzing the color frames, we managed to discover that the cathode flame consists of two parts: a very bright internal part and a wider external part. We saw small bright spots on the anode. Figure 4 shows the calculation results of the radial temperature distribution in the discharge column depending on the current and the mass flow rate of the plasma producing gas. With the increase in the current and the mass flow rate, the arc column temperature increases. Figure 5 shows the frame of the heating spot in the arc burning zone. We clearly see that the heating spot is nonuniform in the color temperature and consists of a group of domains and of little bright points. We performed the calculations on the basis of the red channel. We recalculate the temperature into the thermodynamic one [12–16]. The dimensions of the little bright points might be taken as those of the cathode spot: about 1.0–1.3 mm. The dimension of the particular point measured from the frame equals 0.15 mm.

The diffuse glow around the heating spot is caused by the highlight from the welding arc column. To verify the supposition that the bright domains in the heating spot are the anode spots, we perform PC processing of the image in the different channels. Figure 6 shows the photograph of the welding arc with the cathode and the anode zones in the gray scale for the red, green, and blue channels. The bright domains (the cathode and anode spots) are clearly seen in the blue channel (the blue range of the visible spectrum). The color negative clearly shows the most heated domains in the cathode and the anode arc zones, thus making

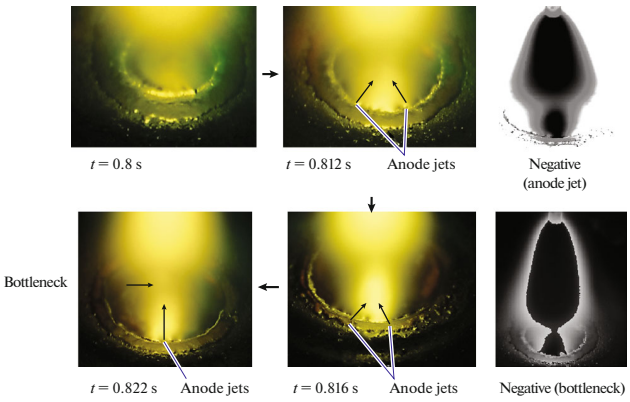

Fig. 3. Occurrence of the anode jets in the heating spot and of the bottlenecks.

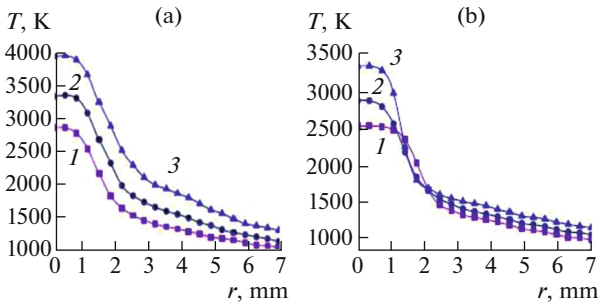

Fig. 4. Temperature distribution in the anode domain depending on the current (a) and the gas mass flow rate (b): (a) *1*, 15 A; *2*, 20 A; *3*, 25 A; (b) *1*, 4 L/min; *2*, 5 L/min; *3*, 6 L/min.

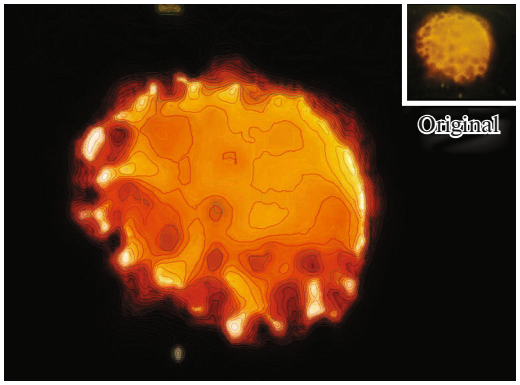

Fig. 5. Map of the brightness temperatures over the heating spot at the arc current 55 A.

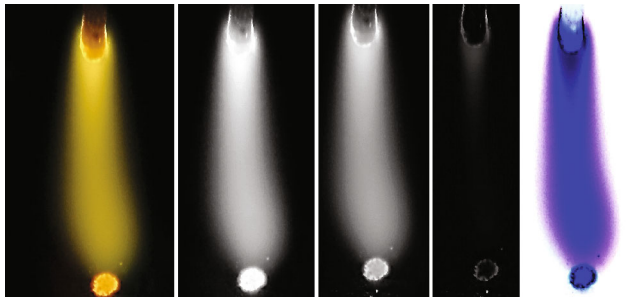

Fig. 6. Total view of the welding arc in the different channels and the color negative.

it possible to take them as the cathode and the anode spots. We calculated all the temperature charts of the heating spot (Fig. 5) with the gray coefficient of 0.42. Note that the temperature range in the red channel is 1260–3520 K and, in the green channel, it is 1400–2600 K. Here, the overload (pinning) was observed in the red channel for the brightest points. The total dynamic range in the heating spot equals 800–3500 K for a single experiment.

DISCUSSION

We should consider the obtained results in the two aspects: physical and methodological. From the standpoint of the physics of the welding arc discharge burning, the data analysis makes it possible to refine certain peculiarities of existence of the discharge. In particular, within the transient regime (the ignition regime and up to the beginning moment of melting), the welding arc discharge has two forms of arc conjunction: diffusion and contraction. The cathode spot, the anode spot, and the arc column zone images of the discharge obtained by means of the digital cameras provide information on the visible wavelength range. Here, we might clearly see (Figs. 2, 3) the characteristic areas within the anode domain of the heating spot: the anode spots, the plasma jets (various length flames) originating from these spots, the diffusion discharge conjunction without visible current lines, and the contraction discharge conjunction with a string current channel. With the cathode jet elongation (with the current increase), we see a displacement, from the anode to the cathode, of the brighter zone occurring due to interaction of the cathode and the anode jets (Fig. 3). It is clearly seen that the anode jets flow out of the common melt dish occurring after significant heating (Fig. 3).

In the experiment with the frame repetition rate of 0.16 ms, we see the column contraction in the anode zone. In all probability, it is caused by the fact that the magnetic pressure in the arc is close to its gas-dynamic pressure [2], thus resulting in column contraction in the anode zone at the arc conjunction point and also in intensive overheating of the molten metal dish accompanied by the anode jet blowout to wards the arc column. Note the important fact registered in the present studies: it is essential to account for the thermal pattern when calculating the metal heating and melting, i.e., the clearly pronounced nonuniformity of the thermal state of the heating spot (Figs. 5, 6). The temperature scatter in the heating spot ranges from 800 to 3500 K at the arc current of 55 A (Fig. 5). Note that this range takes place under the absence of essential disturbing factors such as molten metal movement, current, and voltage oscillations. Here, the temperature in the arc column in the anode zone has a Gauss distribution and depends on variations of the current and the gas mass flow rate (Fig. 4).

The obtained temperature distributions in the arc column for the current of 10–25 A are in good agreement with [7, 10, 14, 15, 20] but contradict [2, 12], because in [2, 12], the welding arc was investigated within the current range 150–300 A. Then, [7] presents a review of the different works aimed at temperature measurement in the welding arc column within the current range of 14–100 A; here, the temperature scatter is from 4000 up to 16000 K. The authors of [7, 16] associate this fact with the different experimental conditions. The majority of authors do not specify the temperature dependencies of the spectral coefficients at the thermal equilibrium that they apply in their calculations for the three states of the argon ionization (1, ArI, $\lambda = 696.5$ nm; 2, ArII, $\lambda = 480.6$ nm; 3, ArII, $\lambda = 333.6$ nm). For example, the temperature of the plasma emitting the ArIII lines exceeds essentially the normal temperature for the ArI lines [1, 2, 7, 16]. The thoroughness of the measurements and good result reproducibility (in the majority of works, the authors refer to these facts) do not solve the problem. In the actual plasma object and in the registering equipment, noises are always present. These noise spectra and the methods of their averaging during data registration and processing are still unknown. All the above-stated information poses the task of refining the total methodology of the temperature determination in the low-ampere arc column both in the present work and in the works of other authors [7, 10, 14, 15, 20]. In general, at the present stage, we can certify that, after the statistical processing of more than 100 images of the arc within the current range 5–100 A, the thermal conditions in the heating spot directly on the metal surface is nonuniform and does not relate to the theoretically normally distributed heat source engaged for the thermal calculations. Figure 6 shows the anode spots located over the boundary of the heating spot and clearly seen in the blue wavelengths and in the color negative. The blue wavelength range is near the ultraviolet range, 100–400 nm. Comparison of the arc image frames taken at different wavelengths shows that usually, with a wavelength increase, the dimensions of

the glowing domains decrease due to the nonmonotonicity of the Plank distribution over the wavelengths.

The authors of [20] show that, in the TIG and A-TIG welding, one should differentiate the action of the total thermal heating spot from that of the anode spots because it is the anode spots that govern the thermal state and the hydrodynamics of the welding dish. The sizes of the anode spots and of the thermal heating spot will govern the influence of the Lorentz force, the Marangoni effect, and the Archimedes force on the hydrodynamic processes in the dish. Figure 6 shows that, on the total thermal heating spot on the metal surface, the thermo-capillary processes cause development of a nonuniform temperature distribution; then, the anode spots are located over the heating spot edges. The spatial size of the anode domain with the spots and the anode flame are fixed well in the color negative.

CONCLUSIONS

(1) The dynamic range of the inexpensive digital cameras (like ά SONY 350, Canon 550d-18-50) makes it possible to obtain high-quality images of the various domains of the welding arc and to investigate the processes in the visible and the infrared arc spectrum wavelengths with use of the respective light filters.

(2) We discovered that the heating spot of a tungsten inert gas welding arc burning in the argon medium is characterized by a nonuniform distribution of the temperature fields over the surface.

(3) We show that, for the transient regimes, the anode spots in the welding arc are located at the edges of the heating spot.

REFERENCES

1. Kesaev, I.G., *Katodnye protsessy elektricheskoi dugi* (Cathodic Processes of Electric Arc), Moscow: Nauka, 1968.
2. Finkelnburg, W. and Maecker, H., Elektrische Bogen ung thermisches Plasma, in *Handbuch der Physik*, Berlin: Springer, 1956, vol. 22.
3. Zykova, N.M., Kantsel', V.V., Rakhovskii, V.I., et al., *Zh. Tekh. Fiz.*, 1970, no. 11, p. 2361.
4. Mesyats, G.A., *Ektony v vakuumnom razryade: proboi, iskra, duga* (Ectons in a Vacuum Discharge: Breakdown, Spark, and Arc), Moscow: Nauka, 2000.
5. Londer, Ya.I. and Ul'yanov, K.N., *High Temp.*, 2014, vol. 52, no. 6, p. 787.
6. Gladkov, E.A. and Perkovskii, R.A., *Svar. Proizvod.*, 1995, no. 4, p. 21.
7. Leskov, G.I., *Elektricheskaya svarochnaya duga* (Electric Welding Arc), Moscow: Mashinostroenie, 1970.
8. German, V.O., Glinov, A.P., Golovin, A.P., Kozlov, P.V., and Lyubimov, G.A., *Plasma Phys. Rep.*, 2013, vol. 39, no. 13, p. 1142.
9. Lazorenko, Ya.P., Shapovalov, E.V., and Kolyada, V.A., *Avtom. Svarka*, 2011, no. 11, p. 24.
10. Li, P.J. and Zhang, Y.M., *Weld. Res. Suppl.*, 2000, no. 9, p. 252.
11. Weglowski, M.S., *Achiev. Mater. Manuf. Eng.*, 2007, no. 12, p. 519.
12. Asinovskii, E.I. and Batenin, V.M., *Teplofiz. Vys. Temp.*, 1965, vol. 3, no. 4, p. 530.
13. Inoue, K., *Trans. JWRI*, 1981, no. 10, p. 13.
14. Ogawa, Y., *Soc. Instrum. Control Eng.*, 2008, vol. 47, p. 65.
15. Ogawa, Y., *Sci. Technol. Weld. Joining*, 2011, vol. 16, no. 1, p. 16.
16. Lochte-Holtgreven, W., *Usp. Fiz. Nauk*, 1960, no. 3, p. 522.
17. Shaw, C.B., *Weld. J.*, 1975, vol. 54, p. 33.
18. Makoveev, A.O., *Vestn. Yugorsk. Gos. Univ.*, 2012, no. 2, p. 59.
19. Goryachev, S.V., Peletskii, V.E., and Chinnov, V.F., *High Temp.*, 2010, vol. 48, no. 1, p. 35.
20. Kovalenko, D.V., Krivtsun, I.V., Demchenko, V.F., and Kovalenko, I.V., *Avtom. Svarka*, 2010, no. 12, p. 5.

Translated by I. Dikhter